Available online at www.eccomasproceedia.org
Eccomas Proceedia COMPDYN (2025) 5642-5652

ECCOMAS
Proceedia

COMPDYN 2025
10th ECCOMAS Thematic Conference on
Computational Methods in Structural Dynamics and Earthquake Engineering
M. Papadrakakis, M. Fragiadakis (eds.)
Rhodes Island, Greece, 15-18 June 2025

GENERALISED PASSIVE STATE-DEPENDENT SWITCHES

Yuan. Li[1], **Emily. Nar**[1], **and Jason Zheng. Jiang**[1]

[1] School of Electrical, Electronic and Mechanical Engineering, University of Bristol, UK, BS8 1TR
e-mail: yuan.li@bristol.ac.uk; gl22021@bristol.ac.uk; z.jiang@bristol.ac.uk

Abstract

State-switched absorbers, introduced in the 1990s, can instantly alter their dynamic properties based on their current state, providing a broader effective bandwidth compared to traditional absorbers. While the switchable properties can be implemented semi-actively, requirements of control systems compromise their reliability and durability. Passive hydraulic components present a promising alternative by switching based on flow patterns or pressure levels (i.e., hydraulic states), such as a floating decoupler switching on flow volume in an engine mount, a check valve switching on flow rate (flow direction) and a blow-off valve switching on pressure level in an automotive suspension. However, existing passive hydraulic state-dependent switch components have two restrictions: 1) there is no component which can passively switch depending on flow acceleration; 2) current flow-dependent components switch relying on the local state of the components (flow volume or flow rate passing through the components), unlike existing pressure-dependent switch components which could switch based on generalised state, i.e., the pressure at any point in the system. To address the two restrictions, this work proposes three novel passive flow-dependent switch component designs. Using these designs, the switching mechanism can 1) depend on flow acceleration; 2) depend on the generalised flow state of the absorber, without being constrained to local states. Together with the existing pressure-dependent switch components, the inclusion of three flow-dependent switch components can fundamentally enlarge the achievable dynamic properties of state-switchable absorbers. To demonstrate the potential of the proposed designs, this work presents a case study on enhancing inerter-based absorber design using state-dependent switches for building seismic protection.

Keywords: Vibration Suppression, Passive state-switchable absorber, Inerter, Seismic, Hydraulic absorber

doi: 10.7712/120125.128 9.25428

1 INTRODUCTION

Design of vibration absorbers is crucial for ensuring safety, dynamic performance and longevity of engineering structures. State-switched absorbers, originally proposed in the 1990s for application in underwater acoustic transducers, realised using piezoelectric material [1], have been found to provide enhanced vibration control. These systems can instantaneously alter their dynamic properties (e.g., mass/inertance, stiffness, or damping) dependent upon its current state, leading to a broader effective bandwidth than traditional absorbers [2]. For example, a switchable-stiffness absorber can change the system's resonance instantaneously, outperforming a conventional absorber in reducing seismic responses [3]; an automotive shock absorber equipped with switchable damping, between hard and soft, can more effectively tackle the comfort-handling trade-off over a conventional damper [4].

While state-switched properties can be implemented using semi-active means, requirements of control systems to operate compromise their reliability and durability. A promising alternative is to use passive hydraulic components which can easily switch corresponding to different hydraulic states, i.e., different pressure level/flow patterns. Example passive hydraulic state-dependent switch components include a floating decoupler for a hydraulic engine mount [5], which switches depending on the flow volume (denoted as flow-volume-dependent switch component in this work); a check valve and a blow-off valve for automotive shock absorbers [6], where a check valve switches depending on the flow direction/flow rate (denoted as flow-rate-dependent switch component) and a blow-off valve switches depending on the pressure level (denoted as pressure-dependent switch component). The combination of these components can lead to significant performance advantages, such as in [4]. However, by reviewing the switching function of these state-of-the-art passive hydraulic state-dependent switch components, there are two restrictions existing: 1) there is no component which can passively switch depending on flow acceleration; 2) current flow-dependent switch components switch relying on the local state of the components (flow volume or flow rate passing through the components), unlike pressure-dependent switch component which could switch based on generalised state, i.e., the pressure at any point in the system. For example, two typical schematics of a blow-off valve are illustrated in Figure 1(a1) and (a2). Such valve will open or close the flow path when the inlet pressure P_1 exceeds a predetermined threshold set by the pre-loaded spring. This operation corresponds to the two design variations illustrated in Figure 1(a1) and (a2) respectively. It is important to note that inlet pressure P_1 is a local state. Figure 1(b1) and (b2) presents the schematic of a pressure-compensated valve [7]. Such valve opens (Figure 1(b1)) or closes (Figure 1(b2)) depending on the generalised states P_i, P_j, because the chambers A and B can be connected with any other parts of the system which have the pressure P_i, P_j. Note that the chamber A or B could also be open to the atmosphere.

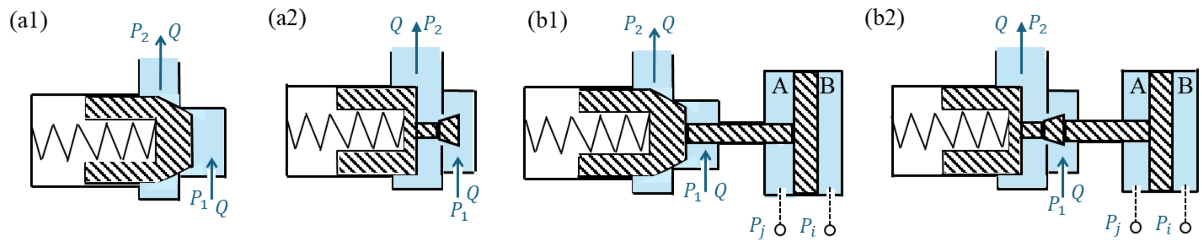

Figure 1: (a1) - (a2): typical schematic representation of a blow-off valve, where the valve opens/closes depending on the local pressure P_1. (b1) - (b2): typical schematic of a pressure-compensated valve, where the valve opens/closes depending on any pressure state in the system (P_i, P_j).

To address the aforementioned restrictions, this work proposes three novel passive hydraulic flow-dependent switch component designs. These designs can 1) allow the switching depending on all flow state including flow acceleration; 2) enable the switching mechanism to transition to the generalised flow state of the absorber, without being constrained to local states. Together with the existing pressure-dependent switch components, the inclusion of three flow-dependent switch components can allow a hydraulic absorber to alter their dynamic properties based on any generalised state (pressure and flow) within it. This will fundamentally enlarge the achievable dynamic properties of state-switchable absorbers. To demonstrate the potential of the proposed designs, this work presents a case study on enhancing inerter-based absorber design using state-dependent switch components for building seismic protection.

2 NOVEL FLOW-DEPENDENT SWITCH COMPONENTS

This section presents the design concepts of the proposed three novel flow-dependent switch components, as illustrated in Figure 2 and the working principle detailed as follows:

- **Flow-volume-dependent switch**: Figure 2(a1) and (a2) illustrate the symbol and schematic diagram for the novel flow-volume-dependent switch component, where $\int Q_i$ is the flow volume accumulated at any point of interest within the absorber, as long as the lower piston-cylinder is positioned at that point. Q denotes the flow to be 'switched on' or 'off'. As shown in Figure 2(a1), when $\int Q_i$ is smaller than zero, the piston of the lower piston-cylinder moves left, pushing the upper valve spool left and closing the flow path Q; when $\int Q_i \geq 0$, the flow path remains open. By altering the inlet and outlet positions of the upper spool valve, the switching condition will be reversed, i.e., when $\int Q_i \leq 0$, the flow path stays open (otherwise closed).

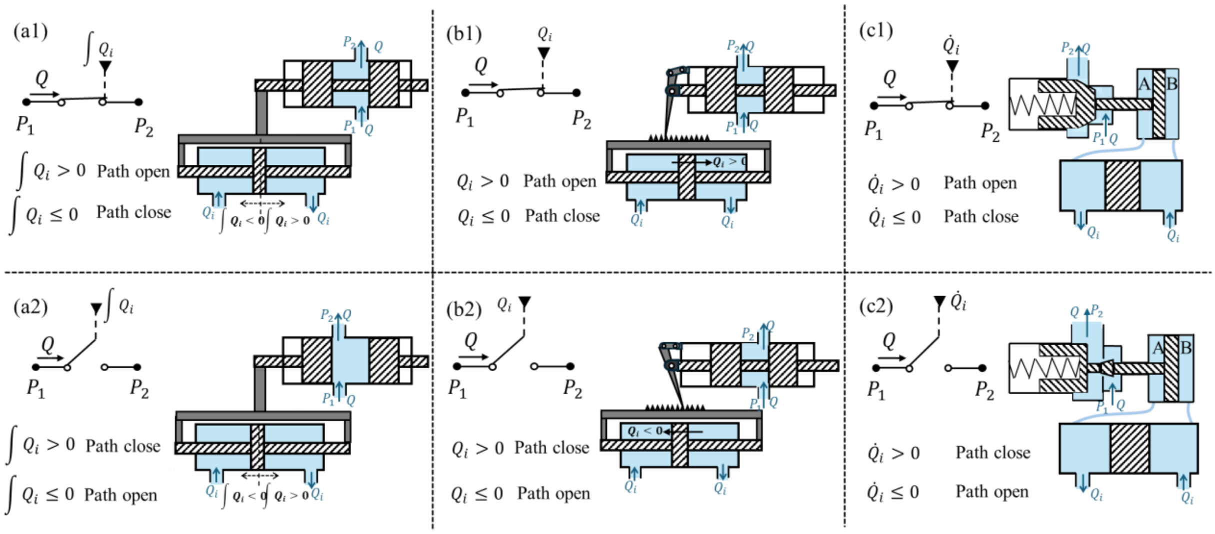

Figure 2: Symbols and schematics of: (a1) - (a2): flow-volume-dependent switch components; (b1) - (b2): flow-rate-dependent switch components; (c1) - (c2): flow-acceleration-dependent switch components.

- **Flow-rate-dependent switch**: The corresponding symbol and the schematical designs are shown in Figures 2(b1) and (b2). Here, the switching variable, i.e., flow rate Q_i, can be any flow rate within the absorber. This is different from a typical check valve of which the switching variable is the local flow through the valve. This component has a rack-lever mechanism between the lower piston and the upper valve spool. Take Figure 2(b1) as an example, when the piston moves left ($Q_i < 0$), the rack forces the lever to change the orientation which will push the spool to close the flow path Q.

- **Flow-acceleration-dependent switch**: Figures 2(c1) and (c2) presents the symbol and the schematical design of the novel flow-acceleration-dependent switch component. Such designs utilise the pressure-dependent switch components (introduced in Figure 1) and a cylinder with a moving mass in it. Assuming the mass is frictionless, if there is a flow acceleration $\dot{Q}_i$, it will cause an acceleration of the moving mass, leading to a pressure difference at the two sides of the mass. Since the two sides of the mass are connected with the pressure-dependent switch valve (Chambers A and B), the pressure difference will cause the valve to be open or closed. For example, if $\dot{Q}_i > 0$, the pressure on the left side of the moving mass is smaller than the right side. Then the pressure in the Chamber B of the pressure-dependent switch valve is larger than that of Chamber A. Such pressure difference will open the flow path through the pressure-dependent switch valve. Similar to the flow-volume-dependent and flow-rate-dependent switch components, the switching variable $\dot{Q}_i$ can be any flow acceleration within the absorber, as long as the lower piston is located at the specific point within the absorber.

3 MODELLING ELEMENTS AND MECHANICAL-ELECTRICAL ANALOGY

There are numerous design possibilities for vibration absorber systems considering components from multiple domains (e.g., mechanical, hydraulic, pneumatic, electrical). Traditional vibration absorber design approaches can only explore limited possibilities, of which the performance is away from optimal. Rather than focusing on a restricted number of designs, since the 2000s, network-synthesis based approaches, such as the structure-immittance approach [8] and a graph-based methodology [9], have been applied for absorber design. Such approaches facilitate the identification of optimal absorber properties represented by networks consisting of idealised modelling elements. These modelling elements are simple and linear but represent the essential properties of physical components. The first three rows of Figure 3 display traditional modeling elements in mechanical and hydraulic domains. Specifically, mechanical modeling elements damping (c), stiffness (k), and inertance (b) [10], are analogous to hydraulic modelling elements resistance (R), compliance (C), and inertance (I), respectively. This analogy is given by mapping a mechanical force F to a hydraulic pressure difference ΔP and a mechanical relative velocity Δv to a hydraulic flow rate Q [10]. This is a typical mechanical-hydraulic analogy because a common device transferring mechanical and hydraulic characteristics is a hydraulic piston cylinder (see Section 4.4 for more details).

The properties of the novel hydraulic state-dependent switch components introduced in Section 2 can also be represented as modeling elements. Building on the mechanical-hydraulic analogy, their mechanical counterparts can also be represented, as shown by rows four and five in Figure 3. More specifically, in the hydraulic domain, the state-dependent switch modelling element is generalised to switch depending upon a switching variable SV_H, which could be either a pressure difference (ΔP_{ij}), a flow volume ($\int Q_i$), a flow rate (Q_i), or a flow acceleration ($\dot{Q}_i$). Analogously, in the mechanical domain, the state-dependent switch modelling element could switch based on the switching variable SV_M, which could be either a force (F_i), a displacement ($\int \Delta v_{ij}$), a velocity (Δv_{ij}) or an acceleration ($\Delta \dot{v}_{ij}$). It is important to note that a subscript ij denotes any point in the network (mechanical or hydraulic).

Following the definition in Figure 2, the symbol of the hydraulic state-dependent switch element in row four of Figure 3 represents that if SV_H >0, the flow path will close, i.e., the flow passing through the component $Q = 0$; if SV_H ≤0, the flow path will open, i.e., $\Delta P = P_1 - P_2 = 0$. To mathematically model this switching function, if SV_H >0, the element can be approximated to be a very high hydraulic resistance (denoted as R_∞), resulting in approximately zero flow Q; when SV_H <0, the element has no resistance, leading to $\Delta P = P_1 - P_2 = 0$. A smooth function is used to approximate the switching between R_∞ and 0, as shown in row four of Figure 3, where κ controls the sharpness of the switching transition and is defined as $\kappa = 4/W$ (W is the transition width). The selection of those values is based on the specific application and the switching variable considered. An example of the smooth function approximating a flow-volume-dependent switch element is illustrated in Figure 4(a). For the hydraulic switch element in row five of Figure 3 (if SV_H >0, the flow path opens otherwise the path closes), a different smooth function would need to be considered to approximate the switching, giving a zero resistance if SV_H >0 and a high resistance if SV_H ≤0.

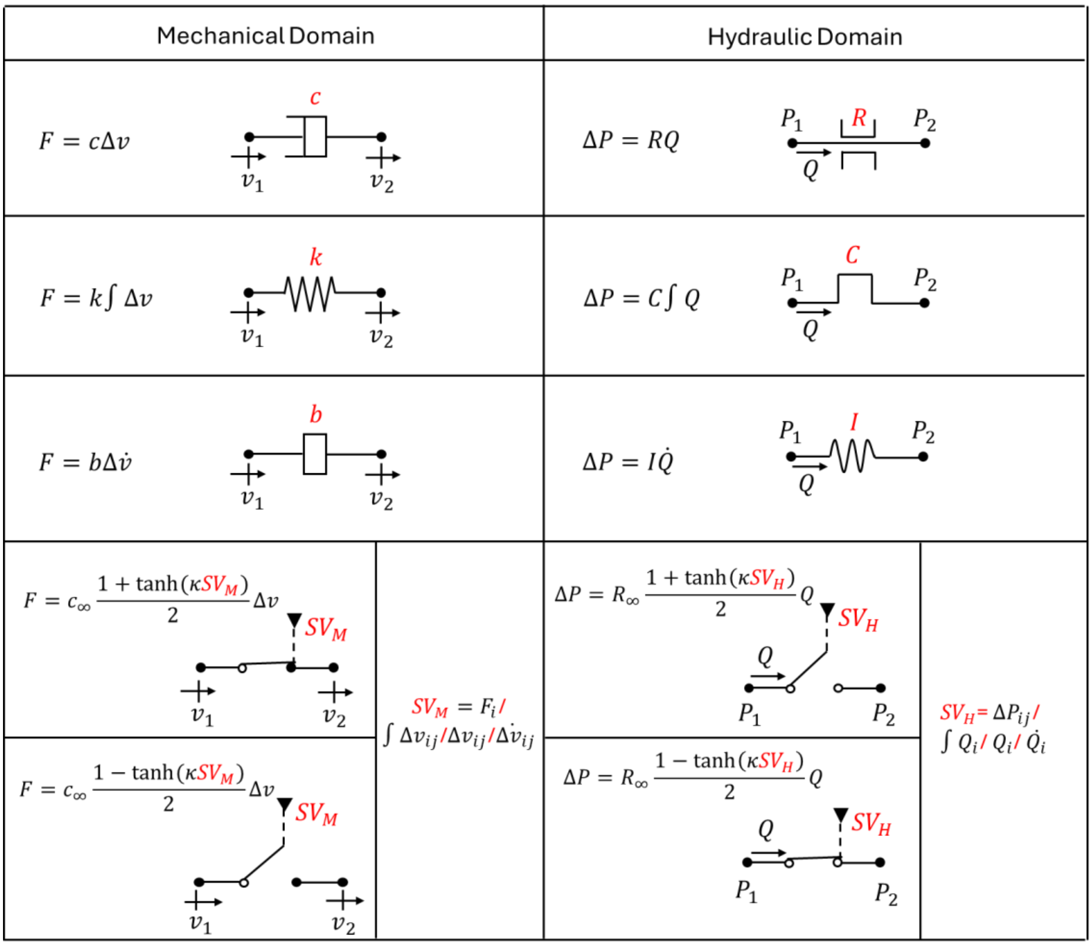

Figure 3: Typical and new state-dependent switch modelling elements in mechanical and hydraulic domain.

Since the analogy allows a force F mapped to a pressure difference ΔP and a relative velocity Δv to a flow rate Q, similar smooth functions can be used to approximate the mechanical state-dependent switch elements. For example, $Q = 0$ (i.e., flow path closes, equivalent to a high hydraulic resistance) is analogous to $\Delta v = 0$. In mechanical domain, a rigid connection gives $\Delta v = 0$, i.e., the element can be approximated as a very high mechanical damping c_∞. Note that to represent a rigid connection in mechanical domain, the switch symbol shows ‘connected’, as illustrated in row four of Figure 3. If $\Delta P = 0$ (i.e., flow path opens, equivalent to zero resistance) is analogous to $F = 0$, i.e., there would be no mechanical connection which is equivalent to a zero-damping effect in the mechanical domain. An example of the smooth function approximating a displacement-switchable element is illustrated in Figure 4(b).

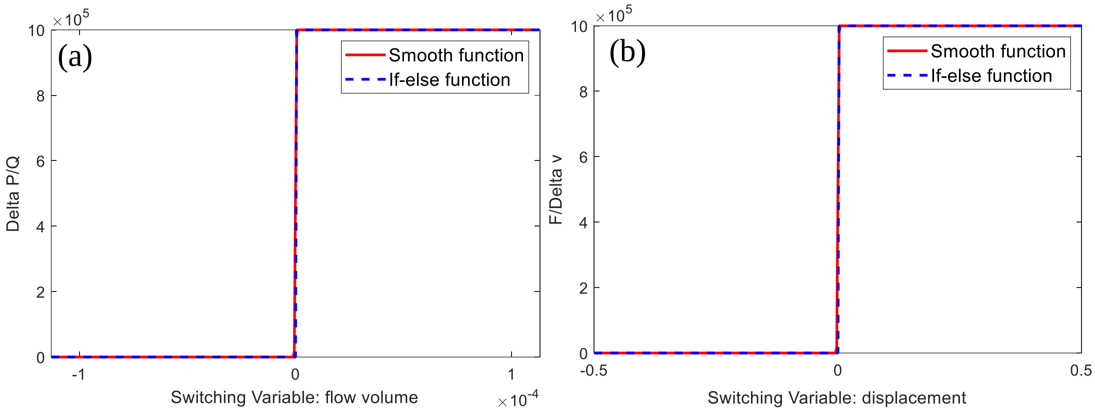

Figure 4: Comparison between the approximate smooth function and if-else function for (a) a hydraulic flow-volume-dependent switch modelling element ($\int Q_i > 0$, path close, otherwise open); (b) mechanical displacement-switchable modelling element ($\int \Delta v_{ij} > 0$, rigidly connected, otherwise disconnected).

4 CASE STUDY

This section presents a case study in which a hydraulic inerter-based absorber is optimally designed, employing the proposed novel passive state-dependent switch components, to enhance the seismic protection of a three-storey building.

4.1 Three-storey building

A three-storey building, modelled as a lumped mass system, is shown in Figure 5(a). Floor mass, inter-storey damping, and inter-storey stiffness are denoted by M_i, c_i, and k_i, respectively, where $i = 1, 2,$ or 3 pertaining to the building storey level. In this case study, the floor masses are assumed as $M_i = M = 5000\text{kg}$, and the inter-storey stiffness is selected as $k_i = k = 2.2 \times 10^6\text{N/m}$. The inter-storey damping is considered to be $c_i = c = 4.2 \times 10^3\text{Ns/m}$, giving an equivalent damping ratio of 2%. A vibration absorber is installed between the ground and the first storey of the building to provide seismic protection of the building.

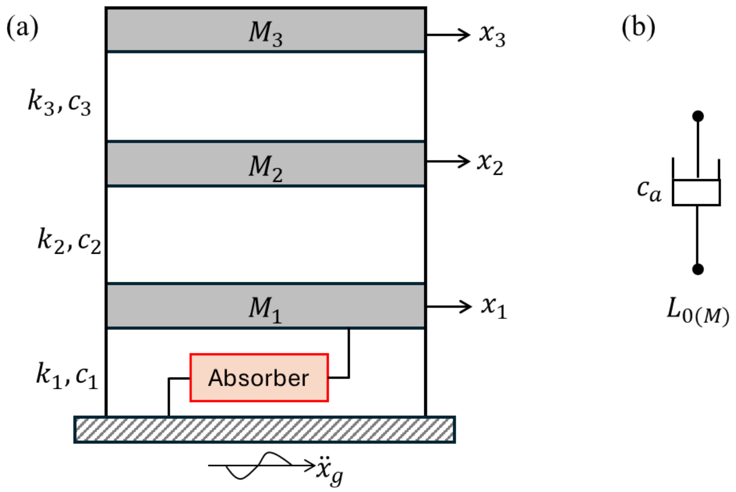

Figure 5: (a) Lumped mass model of an idealised three-storey building, with a vibration absorber installed between the ground and the first storey. (b) Layout of the traditional absorber (denoted as $L_{0(M)}$, and a subscript (M) attached denoting its representation in the mechanical domain).

The equations of motion for the three-storey building model are expressed as follows [8]:

$$\begin{bmatrix} M & 0 & 0 \\ 0 & M & 0 \\ 0 & 0 & M \end{bmatrix} \begin{bmatrix} \ddot{x}_1 \\ \ddot{x}_2 \\ \ddot{x}_3 \end{bmatrix} + \begin{bmatrix} 2c & -c & 0 \\ -c & 2c & -c \\ 0 & -c & c \end{bmatrix} \begin{bmatrix} \dot{x}_1 \\ \dot{x}_2 \\ \dot{x}_3 \end{bmatrix} + \begin{bmatrix} 2k & -k & 0 \\ -k & 2k & -k \\ 0 & -k & k \end{bmatrix} \begin{bmatrix} x_1 \\ x_2 \\ x_3 \end{bmatrix} = -\begin{bmatrix} M & 0 & 0 \\ 0 & M & 0 \\ 0 & 0 & M \end{bmatrix} \begin{bmatrix} \ddot{x}_g \\ \ddot{x}_g \\ \ddot{x}_g \end{bmatrix} - \begin{bmatrix} F_a \\ 0 \\ 0 \end{bmatrix} \quad (1)$$

where x_1, x_2, and x_3 represent the displacements of the first, second, and third storey relative to the ground, respectively; $\ddot{x}_g$ is the ground acceleration caused by the earthquake. F_a is the force exerted by the absorber. Considering a damper as a traditional absorber (as illustrated in Figure 5(b) and denoted as $L_{0(M)}$), F_a is then given by:

$$F_a = c_a.\dot{x}_1 \quad (2)$$

where c_a denotes the damping coefficient of the traditional damper.

4.2 Optimisation problem and candidate design possibilities

In this case study, the dynamic behaviour of the three-storey building is examined under an earthquake excitation, the Northridge Earthquake (M 6.7), which occurred in California in 1994. Inter-storey drifts are chosen as the performance index quantifying seismic damage. While various design criteria for vibration absorbers exist, the design focus of this case study is selected to minimise the peak inter-storey drift, denoting the inter-storey drift for the ith storey x_{di} as

$$x_{di} = x_i - x_{i-1} \quad (3)$$

where $i = 2$, or 3 and $x_{d1} = x_1$. Then, the objective function for optimisation is formulated as:

$$J = \max(|x_{di}|) \quad (4)$$

All absorber designs considered, including those featuring the novel state-switchable components, are optimised to minimise this objective function J. A hybrid optimisation technique is employed, combining Particle Swarm Optimization (*PSO*) and *fmincon* in MATLAB.

In this study, to identify an effective inerter-based absorber for seismic protection, the absorber is redesigned by considering all possible network configurations comprising one inerter, one damper, and one spring element. This yields eight distinct network configurations, as illustrated in Figure 6. Note that the full set of network possibilities considering any pre-determined complexity can be obtained using network-synthesis-based techniques, such as the structure-immittance approach [9] or a graph-based method [10]. Here the full set of networks consisting of one spring, one damper and one inerter is considered as an example. To assess the effectiveness of each network design, the traditional absorber ($L_{0(M)}$, illustrated in Figure 5(b)) is firstly optimised. Subsequently, each linear network configuration, $L_{1(M)} - L_{8(M)}$, is individually substituted in place of the traditional absorber and optimised.

Apart from the linear possibilities, the design possibilities considering state-dependent switch properties are also considered in this case study. Inspired by the velocity-displacement-dependent damper introduced in [4], a state-switchable nonlinear damper, illustrated in Figure 7(a) and denoted as $SL_{0(M)}$, is considered first ('S' denotes 'switchable'). This layout contains a linear damper c, two displacement-switchable and two velocity-switchable components. In addition, to explore potential further enhancements to seismic performance, $SL_{0(M)}$ is substituted in place of the linear damping element (c) in each of eight designs presented in Figure 6, leading to eight state-switchable network designs $SL_{1(M)} - SL_{8(M)}$. Optimisation is then conducted to determine the optimal set of element values that minimise the objective function. Note that here only a very limited set of state-switchable design possibilities ($SL_{1(M)} - SL_{8(M)}$) are considered – more performance benefits can be anticipated if the totality of state-switchable design possibilities (considering any number of modelling elements illustrated in Figure 3) can be fully explored.

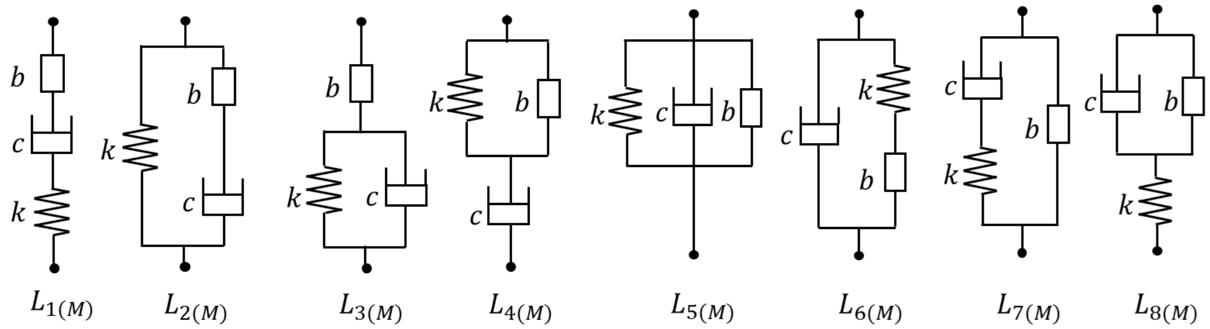

Figure 6: Eight linear inerter-based network design possibilities denoted as $L_{1(M)} - L_{8(M)}$.

4.3 Optimisation results

Following the design problem formulated in Section 4.2, nine linear network design possibilities ($L_{0(M)} - L_{8(M)}$) and nine state-switchable possibilities ($SL_{0(M)} - SL_{8(M)}$) are optimised. The optimisation results are summarised in Table 1, including the performance and parameter settings for all the identified beneficial networks.

Optimised Network Solution	J (mm)	Improv. (%) (over $L_{0(M)}$)	Mechanical Network properties (SI units)
$L_{0(M)}$	5.40	/	$c_a = 2.13 \times 10^5$
$L_{4(M)}$	4.97	7.96	$c = 1.88 \times 10^5, b = 2.18 \times 10^4, k = 9.97 \times 10^3$
$SL_{0(M)}$	4.99	7.59	$c = 5.42 \times 10^3$
$SL_{6(M)}$	4.10	24.07	$c = 5.23 \times 10^3, b = 2.1 \times 10^4, k = 8.33 \times 10^3$

Table 1: Performance and parameter settings for the identified beneficial designs, including optimised traditional damper $L_{0(M)}$, the optimal linear network $L_{4(M)}$, the state-switchable damper $SL_{0(M)}$, and the optimal state-switchable network design $SL_{6(M)}$.

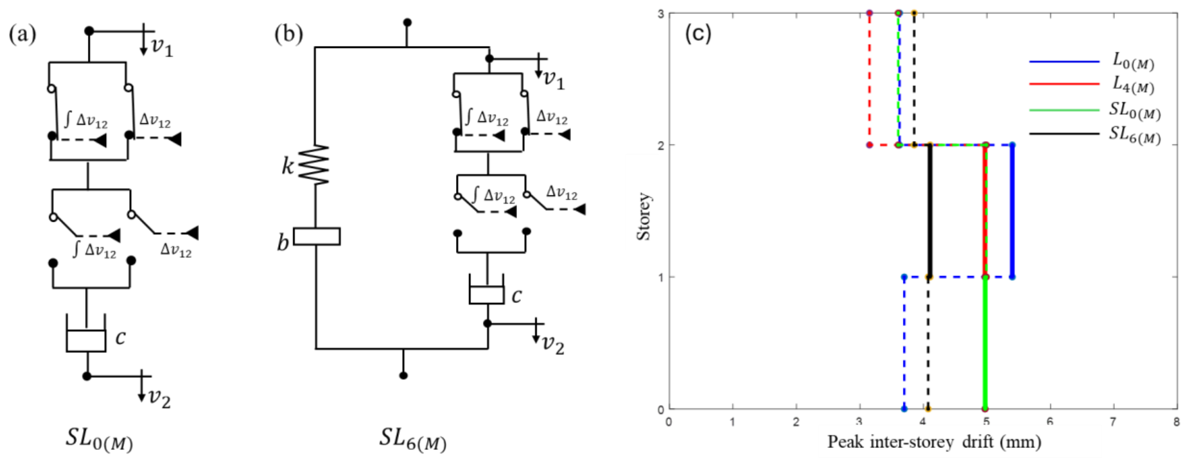

Figure 7: (a) State-switchable damper layout $SL_{0(M)}$, (b) identified optimal state-switchable mechanical network layout $SL_{6(M)}$, and (c) Peak inter-storey drift response of the building, subjected to the Northridge Earthquake.

The linear network design $L_{4(M)}$ is found to provide the best performance among $L_{0(M)} - L_{8(M)}$, reducing the maximum inter-storey drift by 7.4% over the conventional damper $L_{0(M)}$. Similar performance improvement can be obtained with the optimised state-switchable damper

$SL_{0(M)}$. The optimal state-switchable network identified is $SL_{6(M)}$, of which the layout can be seen in Figure 7(b). The parameter settings for $SL_{0(M)}$ and $SL_{6(M)}$ are given in the third and fourth rows of Table 1, respectively. From Table 1, it can be seen that $SL_{6(M)}$ can provide a reduction of 24% in the peak inter-storey drift compared to the conventional absorber $L_{0(M)}$, and a further reduction of 17.5% compared to the best linear network $L_{4(M)}$. This improvement can be visualised in Figure 7(c) which presents the inter-storey drift responses of the building when equipped with the networks $L_{0(M)}$, $L_{4(M)}$, $SL_{0(M)}$, and $SL_{6(M)}$.

4.4 Physical realisation

Despite of the significant performance improvement, the optimal design $SL_{6(M)}$ is represented by a network, i.e., consisting of modelling elements. To enable real-life application of $SL_{6(M)}$, it is necessary to construct a physical device that can realise its network properties. In contrast to the convenience of realising stiffness, damping and inertance mechanically, the physical realisation of mechanical switch components that operate independently of their local state presents significant challenges. To overcome this limitation, this study considers a hydraulic absorber realisation, ultilising the proposed novel hydraulic state-dependent switch components introduced in Section 2. To construct the physical device, this work employs the multi-domain vibration absorber synthesis technique developed in [11], which could allow the optimal network-represented properties to be realised using physical components from multiple domains (hydraulic, pneumatic, mechanical and electrical).

Following [11], $SL_{6(M)}$ must first be converted into an equivalent hydraulic network considering a mechanical-hydraulic coupling device. Here, a hydraulic piston cylinder mechanism can be considered as the coupling, which is also typically used in the hydraulic damper for building seismic protection. Using the piston cylinder, the following coupling equations can be given:

$$F = A\Delta P_{12} \quad \text{and} \quad \Delta v_{12} = \frac{Q_1}{\mathrm{A}} \tag{5}$$

where A is the piston area, F is the force acting on the piston caused by the pressure difference in the two chambers ΔP_{12}, Δv_{12} is the relative velocity of the piston-cylinder, and Q_1 is the flow rate going in/out of the cylinder. It can be seen that the mechanical through variable F is mapped to the hydraulic across variable ΔP_{12}, and that the mechanical across variable Δv_{12} to the hydraulic through variable Q_1. This transformation renders the parallel connections of modelling elements in the mechanical domain to be transferred to series connections of the analogous elements in the hydraulic domain, and vice versa, i.e., the dual. Readers could refer to [11] for more details. The resulting hydraulic network, denoted as $SL_{6(H)}$, is depicted in Figure 8(a). The mechanical modelling elements $c, k,$ and b correspond to the hydraulic modelling elements of resistance (R), compliance (C), and inertance (I), respectively. Furthermore, the mechanical switching variables dependent on displacement and velocity are transformed into hydraulic switching variables dependent on flow volume and flow rate, respectively. Using the piston cross-sectional area found in [12], the mechanical network properties, given in Table 1, can be converted to hydraulic network properties as follows: $R = c/A^2 = 3.67 \times 10^7 \mathrm{kg/sm^4}$, $C = k/A^2 = 5.83 \times 10^7\ \mathrm{kg/s^2m^4}$ and $I = b/A^2 = 1.46 \times 10^6\ \mathrm{kg/m^4}$.

The next step involves constructing a physical device to realise the hydraulic network of $SL_{6(H)}$, which includes the realisation of its modelling element parameter values and their topological arrangements. In this case study, a helical pipe [13], an orifice, and a dual spring device [11] are utilised to realise hydraulic inertance, resistance, and compliance elements, respectively. To realise the flow-rate-dependent and the flow-volume-dependent switch properties, the components presented in Figure 2 are utilised. Figure 8(b) displays a schematic diagram of the physical hydraulic device, realising the network topology of $SL_{6(H)}$. It should be noted that Figure 8(b) only shows the schematic design, not indicating the detailed sizing of each component. To identify the sizing, i.e., physical parameters of each component, an absorber model needs to be developed, capturing the accurate physical behaviour of the device. In such model, the component properties are characterised in terms of physical design parameters, rather than idealised modeling elements adopted in the network configuration. There are different approaches to establish such absorber model, for example, using analytical equations or simulation software's. Integrating the established absorber model into the building model, the design parameters can then be optimised against the objective function. Note that in this paper, this step has not been performed yet and is regarded as the important next step of this work.

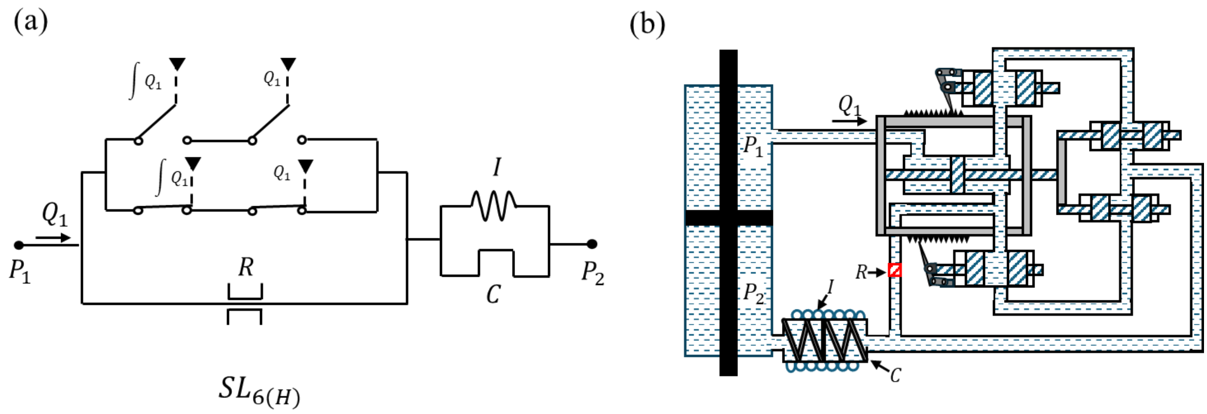

Figure 8: (a) Hydraulic network $SL_{6(H)}$, where the subscript (H) indicates the representation within the hydraulic domain. b) The corresponding physical design schematic realising the topology of $SL_{6(H)}$. Note that this schematic design does not indicate the detailed sizing of each component.

5 CONCLUSION

This work proposes three novel passive hydraulic state-dependent switch components, which can allow a flow path to be open or closed, depending on any generalised flow state (flow volume, flow rate and flow acceleration) within the absorber, not limited to local states. The idealised properties of these components have been represented as modelling elements in hydraulic domain and their mechanical counterparts have been presented following a mechanical-hydraulic analogy. Facilitated by the network synthesis technique and multidomain absorber synthesis method, the beneficial absorber with state-dependent switch properties can be identified in mechanical domain and physically realised using the hydraulic components. This work also presents a case study on seismic protection of a 3-storey building. It has been found that the design with the proposed state-dependent switch properties can further reduce the maximum inter-story drift by 17.5% compared to the optimal non-switchable design (considering a predefined complexity). It should be noted that in this work only a very limited set of design possibilities with flow-volume-dependent and flow-rate-dependent switch properties are considered. One could expect more performance benefits if the totality of the designs with any predefined number and types of the state-dependent switch properties can be fully explored.

REFERENCES

[1] Larson, G. D., & Rogers, P. H. State switched acoustic source. *The Journal of the Acoustical Society of America*, 96(5_Supplement), 3317-3317, 1994.

[2] Cunefare, K. A., De Rosa, S., Sadegh, N., & Larson, G. State-switched absorber for semi-active structural control. *Journal of intelligent material systems and structures*, *11*(4), 300-310, 2000.

[3] Cunefare, K. A. State-switched absorber for vibration control of point-excited beams. *Journal of Intelligent Material Systems and Structures*, 13(2-3), 97-105, 2002.

[4] Nie, S., Zhuang, Y., Wang, Y., & Guo, K. Velocity & displacement-dependent damper: A novel passive shock absorber inspired by the semi-active control. *Mechanical Systems and Signal Processing*, *99*, 730-746, 2018.

[5] Li, Y., Jiang, J. Z., & Neild, S. A. Optimal fluid passageway design methodology for hydraulic engine mounts considering both low and high frequency performances. *Journal of Vibration and Control*, 25(21-22), 2749-2757, 2019.

[6] Reybrouck, K. A non-linear parametric model of an automotive shock absorber. *SAE transactions*, 1170-1177, 1994.

[7] Wang, B., Liu, H., Hao, Y., Quan, L., Li, Y., & Zhao, B. Design and analysis of a flow-control valve with controllable pressure compensation capability for mobile machinery. *IEEE Access*, 9, 98361-98368, 2021.

[8] Zhang S.Y., Jiang J.Z., Neild S.A. Passive vibration control: a structure–immittance approach. *Proceedings of the Royal Society A: Mathematical, Physical and Engineering Sciences*. May 31;473(2201):20170011, 2017.

[9] He, H., Li, Y., Wang, Z., Jiang, J. Z., Burrow, S., Neild, S., & Conn, A. A Graph-based methodology for optimal design of inerter-based passive vibration absorbers with minimum complexity. *Structural Control and Health Monitoring*, *2024*(1), 8871616, 2024.

[10] Smith, M. C. (2002). Synthesis of mechanical networks: the inerter. *IEEE Transactions on automatic control*, *47*(10), 1648-1662.

[11] Li, Y., Zheng Jiang, J., Neild, S. A., & Titurus, B. Multidomain synthesis of optimal vibration suppression systems. *Journal of Mechanical Design*, *145*(11), 111701, 2023.

[12] Kurata, N., Kobori, T., Takahashi, M., Niwa, N., & Midorikawa, H. Actual seismic response-controlled building with semi-active damper system. *Earthquake engineering & structural dynamics*, *28*(11), 1427-1447, 1999.

[13] Liu, X., Jiang, J. Z., Titurus, B., & Harrison, A. Model identification methodology for fluid-based inerters. *Mechanical Systems and Signal Processing*, *106*, 479-494. 2018.